View metadata, citation and similar papers at core.ac.uk
brought to you by CORE
provided by Apollo

Characterisation of glucose related metabolic pathways in differentiated rodent oligodendrocyte lineage cells

Ana I Amaral[1], Mussie G Hadera[2], Joana M Tavares[1], Mark Kotter[1*], Ursula Sonnewald[2,3*]

[1] Wellcome Trust-Medical Research Council Cambridge Stem Cell Institute, Anne McLaren Laboratory, Department of Clinical Neurosciences - University of Cambridge, West Forvie Building, Robinson Way, Cambridge CB2 0SZ, United Kingdom.

[2]Department of Neuroscience, Faculty of Medicine, Norwegian University of Science and Technology, PO Box 8905, 7491 Trondheim, Norway

[3]Department of Drug Design and Pharmacology, Faculty of Health and Medical Sciences, University of Copenhagen, Universitetsparken 2, 2100 Copenhagen, Denmark

Running title: Oligodendrocyte metabolism

Word count: Introduction (921), Materials and Methods (1721), Results (1645), Discussion (1964), Conclusion (109), Acknowledgements (42), References (2041), Figure Legends (1019 + 56 sup figure), Figures (5 + 1 sup figure), Total word count (9528).

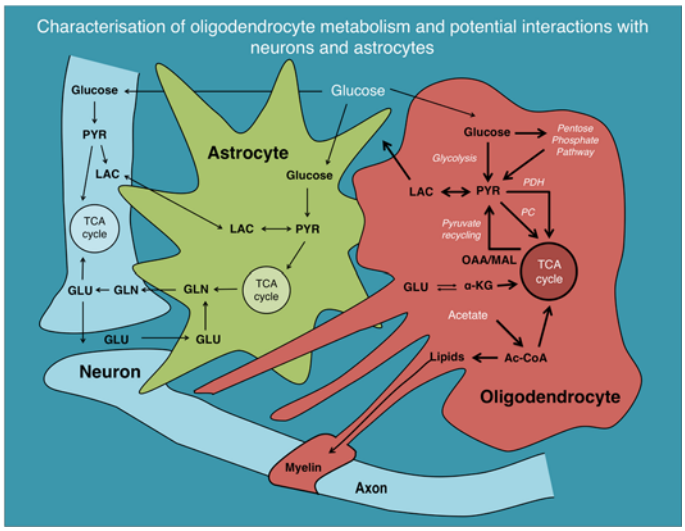

Main points: Oligodendrocytes metabolise glucose via the pentose phosphate pathway to a similar extent as astrocytes. They have avid mitochondrial metabolism, can carboxylate pyruvate, decarboxylate malate and oxaloacetate and metabolise acetate in the mitochondria.

*** Corresponding authors:**

Professor Ursula Sonnewald

Department of Neurosciences, Faculty of Medicine - Norwegian University of Science and Technology, PO Box 8905, MTFS, 7491 Trondheim, Norway

E-mail: Ursula.sonnewald@ntnu.no; Telephone: +4773590492

Dr Mark Kotter

WT MRC Cambridge Stem Cell Institute – Anne McLaren Laboratory, Department of Clinical Neurosciences, University of Cambridge, West Forvie Building, Robinson Way, CB2 0SZ Cambridge, United Kingdom

E-mail: mrk25@cam.ac.uk; Telephone: +44 1223 74747

Abstract

Although oligodendrocytes constitute a significant proportion of cells in the central nervous system (CNS), little is known about their intermediary metabolism. We have therefore characterised metabolic functions of primary oligodendrocyte precursor cell cultures at late stages of differentiation using isotope-labelled metabolites. We report that differentiated oligodendrocyte lineage cells avidly metabolise glucose in the cytosol and pyruvate derived from glucose in the mitochondria. The labelling patterns of metabolites obtained after incubation with [1,2-^{13}C]glucose demonstrated that the pentose phosphate pathway (PPP) is highly active in oligodendrocytes (approximately 10% of glucose is metabolised via the PPP as indicated by labelling patterns in phosphoenolpyruvate). Mass spectrometry and magnetic resonance spectroscopy analyses of metabolites after incubation of cells with [1-^{13}C]lactate or [1,2-^{13}C]glucose, respectively, demonstrated that anaplerotic pyruvate carboxylation, which was thought to be exclusive to astrocytes, is also active in oligodendrocytes. Using [1,2-^{13}C]acetate we show that oligodendrocytes convert acetate into acetyl-CoA which is metabolized in the tricarboxylic acid cycle. Analysis of labelling patterns of alanine after incubation of cells with [1,2-^{13}C]acetate and [1,2-^{13}C]glucose showed catabolic oxidation of malate or oxaloacetate. In conclusion, we report that oligodendrocyte lineage cells at late differentiation stages are metabolically highly active cells that are likely to contribute considerably to the metabolic activity of the CNS.

Keywords: Oligodendroglia, energy metabolism, glucose, ^{13}C, mitochondria, glycolysis, acetate, pyruvate carboxylation.

Introduction

Oligodendrocytes make up a large proportion of the cells in the central nervous system (CNS). Although oligodendrocytes are vulnerable to low energy conditions (Lyons and Kettenmann 1998; Yan and Rivkees 2006), their metabolic properties, including their glucose metabolism, have not been investigated in depth (Amaral et al. 2013). In contrast, the metabolic interactions between neurons and astrocytes, have received considerable attention since their discovery in the 1970′s (van den Berg and Garfinkel 1971). Specifically, the shuttling of glutamine - glutamate - γ-Aminobutyric acid (GABA) between astrocytes and neurons is thought to be fundamentally important for neuronal function. Because neurons themselves are unable to generate essential precursors of glutamate, GABA and aspartate, they depend on the supply of glutamine as a precursor from astrocytes for the production of neurotransmitters (glutamate in 90% of the synapses, and GABA in 5%) (Attwell and Laughlin 2001). In this context, glucose plays a central role as the key molecular building block that is used to synthesize glutamate, GABA and aspartate.

Glucose is primarily metabolised to pyruvate via glycolysis in the cytosol. Stepwise conversion of a single glucose molecule into two pyruvate molecules generates two molecules of ATP. These reactions are not oxygen dependent. Glucose metabolism can also take an alternative route via a biosynthetic pathway termed *pentose phosphate pathway* (PPP). This complex detour bypasses several steps of glycolysis. In the first, *oxidative phase* of the PPP, NADP+ is converted into NADPH. NADPH acts as a reducing agent that may participate in lipid and steroid synthesis or in the regeneration of glutathione and thioredoxin, which are involved in the cell′s defense mechanism against oxidative stress. In the second phase of the PPP, 5-carbon sugars are non-oxidatively synthetised. The PPP joins the glycolytic pathway at the level of glyceraldehyde-3-phosphate (GA3P) and fructose-6-phosphate (fructose-6P).

Fructose-6P is subsequently converted into pyruvate, which constitutes the endpoint of both glycolysis and the PPP.

In the presence of oxygen, the pyruvate produced by glycolysis or by the PPP can be converted to acetyl CoA by the pyruvate dehydrogenase (PDH) complex, and subsequently metabolised in the mitochondrial tricarboxylic acid (TCA) cycle, to further produce ATP via coupling to the mitochondrial electron transport chain. Alternatively, pyruvate can be (reversibly) converted into lactate in the cytosol, which results in the production of NAD+ from NADH. Net synthesis of TCA cycle intermediates and related compounds, including glutamate and glutamine, depend on *anaplerotic* replenishment of intermediates in the TCA cycle. In the brain, this is mediated by pyruvate carboxylase (PC) (Patel 1974). Pyruvate carboxylation was shown to be absent in neurons, but present in astrocytes (Cesar and Hamprecht 1995; Hertz et al. 1980; Shank et al. 1985) (for review see Sonnewald and Rae 2010). Consequently, neurons are thought to depend on astrocytes as an external source of glutamine for the production of neurotransmitters. Conversion of pyruvate by PC generates a 'new' molecule of oxaloacetate. Oxaloacetate may subsequently condense with acetyl CoA to synthesise the TCA cycle intermediate citrate, which, after several steps, is converted to α-ketoglutarate, from which glutamate can be formed by transamination or deamination. In a subsequent step, glutamine synthetase, which is known to be expressed in astrocytes (Martinez-Hernandez et al. 1977; Norenberg and Martinez-Hernandez 1979), is able to convert glutamate into glutamine (see Figure 1 in Amaral et al. 2013).

In the grey matter, glutamate, released from neuronal synapses during glutamatergic neurotransmission, is mainly taken up by astrocytes (Gegelashvili and Schousboe 1997; Gegelashvili and Schousboe 1998). The drain of glutamate from signalling neurons is subsequently compensated by a reverse flow of glutamine from astrocytes back to the neurons. This cross flow of glutamate and glutamine is often referred to as the glutamate –

glutamine cycle (McKenna et al. 2012) (see Figure 1 in Amaral et al. 2013). Because glutamine released by astrocytes also functions as a precursor for the production of the inhibitory neurotransmitter GABA via conversion to glutamate (Reubi et al. 1978; Sonnewald et al. 1993b), metabolic interactions between astrocytes and neurons are thought to consist of a glutamate-glutamine and a glutamine-glutamate-GABA cycle.

How can oligodendrocytes contribute to the metabolic interactions in the CNS? We have argued that, instead of being restricted to closed-loop interactions between astrocytes and neurons, inter-cellular shuttling of metabolites may occur between all three major cell groups of the CNS: neurons, astrocytes, and oligodendrocytes (Amaral et al. 2013). The limited understanding of the metabolic role of oligodendrocytes in the brain was further highlighted in two recent studies, which, for the first time, proposed a link between glycolytic metabolism in oligodendrocytes and axonal integrity and function (Funfschilling et al. 2012; Lee et al. 2012).

The aim of the present study was to elucidate basic metabolic pathways for glucose catabolism and the anaplerotic replenishment of TCA cycle intermediates in oligodendrocytes. For this purpose we incubated primary cultures enriched for mature oligodendrocytes in medium containing [1,2-^{13}C]glucose, [1,6-^{13}C]glucose, [1-^{13}C]lactate or [1,2-^{13}C]acetate and analysed cell extracts and medium using mass spectrometry or nuclear magnetic resonance (NMR) spectroscopy. We found that oligodendrocytes have extensive PPP activity. Furthermore, oligodendrocytes were able to anaplerotically replenish the TCA cycle, via pyruvate carboxylation, and cataplerotically recycle pyruvate. Our data also show that oligodendrocytes are able to convert [1,2-^{13}C]acetate into acetyl CoA. Our results establish hallmarks of the cellular metabolism of oligodendrocytes under physiological conditions. They may also be useful for future studies investigating altered oligodendrocyte function and injury in diseases that involve glutamate toxicity and impaired mitochondria

function, including e.g. hypoxic-ischemic damage, and Multiple Sclerosis (MS) (Kostic et al. 2013; Mifsud et al. 2014; Pitt et al. 2000; Simonishvili et al. 2013).

Materials and Methods

Materials

Cell culture reagents were purchased from Sigma (Dorset, UK) - Dulbecco's Modified Eagle's Medium (DMEM), Minimum Essential Medium Eagle (MEM), L-Glutamine, poly-L-lysine (PLL), papain - or Life Technologies (Paisley, UK) - fetal bovine serum (FBS), penicillin-streptomycin (pen-strep), trypsin-EDTA, phosphate buffered saline (PBS). ^{13}C-labelled compounds were obtained from Cambridge Isotope Laboratories, MA, USA. The mass spectrometry derivatization reagents MTBSTFA (*N*-methyl-*N*- (tert - Butyldimethylsilyl) trifluoroacetamide), MSTFA (*N*-Methyl-*N*-(trimethylsilyl) trifluoroacetamide) and the t-BDMS-Cl (tert-butyldimethylchlorosilane) were purchased from Regis Technologies, Inc. (Morton Grove, IL, USA). All other chemicals were of the purest grade available from Sigma (Dorset, UK).

Preparation of primary oligodendrocyte precursor cell (OPC) cultures

Primary mixed glia cultures were isolated from neonatal Sprague Dawley rat (postnatal day 0–2) forebrains following a standard protocol (Baer et al. 2009). Pups were euthanized according to "Schedule 1" regulations from the Home Office Animal Procedures Committee UK. Cells were cultured for 10-15 days in DMEM supplemented with 10% FBS, 1% pen-strep) and 4 mM glutamine, and kept under a humidified atmosphere at 37°C and 7% CO_2. Oligodendrocyte precursor cells (OPCs) were subsequently isolated using a step-based shake-off protocol and cultured in Sato's medium on PLL-coated plates (Baer et al. 2009). To induce differentiation, OPCs were cultured in Sato's medium supplemented with 0.5% fetal calf serum (FCS). The cell culture medium was replaced by fresh medium at day two of differentiation. For all *in vitro* experiments only cultures with >93% purity (determined based on O4 immunostaining) were used (Figure 1). Quantification of the number of GFAP-positive

cells after 5 days of differentiation, indicated that astrocytes comprised 7-10% of total cells (data not shown).

Preparation of rat cortical astrocyte cultures

Astrocytes were prepared from the same mixed glia cultures used for OPC isolation, following an adapted protocol described in (Amaral et al. 2014). After the shake-off (which eliminates microglia and most oligodendrocytes from the cultures), the remaining cells, highly rich in proliferative astrocytes, were seeded into new T75 flasks (1:3 dilution) using DMEM supplemented with 10% (v/v) FBS, 4 mM glutamine, and 1% (v/v) pen-strep and allowed to reach confluence (approx. 5-7 days). Then, cells were collected with trypsin-EDTA and seeded in 6 well plates at a density of $5x10^4$ cells/well for the [1-^{13}C]lactate experiments. Experiments were performed when cells reached confluence.

Incubations with ^{13}C labelled compounds

Mature OPC cultures (after 5 days in differentiation medium) were cultured in 6 well plates at a cell density of $4x10^5$ cells/well. Prior to incubation, cells were washed once with PBS and incubated with 2 ml Sato's medium prepared from a glucose, glutamine and pyruvate-free DMEM (Sigma D5030) supplemented with 0.5% FCS and 2 mM [1,6-^{13}C]glucose, 2 mM [1,2-^{13}C] glucose + 1 mM glutamine, 2 mM [1,2-^{13}C]acetate + 1 mM glutamine or 5 mM [1-^{13}C]lactate + 2 mM glucose + 1 mM glutamine for 24h. Astrocytes were washed once with PBS and incubated with 2 ml DMEM (Sigma D5030) supplemented with 4 mM [1-^{13}C]lactate + 2 mM glucose, 1 mM glutamine, 1% pen-strep and 1% FBS for 24h. Samples of medium were collected before and after the incubation period and subsequently analysed by mass spectrometry. After the 24h incubation period, cells were washed twice with cold PBS and the intracellular metabolites extracted with 70% ethanol (Amaral et al. 2014). Astrocyte cultures were also incubated for 24h in 2 ml DMEM containing 2 mM D-glucose, 1 mM glutamine,

1% pen-strep and 1% FBS in order to determine glucose consumption and lactate production rates after 24h. Experiments were performed on 9 - 12 samples, which derived from a minimum of three independently generated cultures.

Immunocytochemistry

OPCs were seeded on PLL-coated glass coverslips on 24 well plates ($7x10^4$ cells/well) and fixed after 5 days of differentiation with 4% paraformaldehyde. Cells were stained with an anti-O4 mouse monoclonal antibody (1:200; Sigma, Dorset, UK), anti-myelin basic protein (MBP) rat polyclonal antibody (1:300; Merck Millipore, Hertfordshire, UK) and anti-glial fibrillary acidic protein (GFAP) rabbit polyclonal antibody (1/500; Dako, Glostrup, Denmark). Secondary antibodies conjugated with Alexa Fluor 488 and Alexa Fluor 555 were used to visualize positive cells (1:500; Life Technologies, Paisley, UK). Following immunocytochemistry, cells were mounted with Prolong gold antifade mounting medium (Life Technologies, Paisley, UK). To assess purity and differentiation of oligodendroglia lineage cells in the cultures, the percentage of O4-, MBP- and GFAP- positive cells relative to >100 DAPI-stained nuclei per experiment in randomly selected eye fields was determined. Cells were visualized and digitized at ambient temperature on an LSM 700 confocal microscope (Zeiss, Thornwood, NJ) at 20× magnification using Zen Application software (Zeiss).

Assessment of cell viability

To assess cell viability under the different experimental conditions, the Dead End™ Fluorometric TUNEL System Kit (Promega, Madison, WI) was used according to the manufacturer's instructions. Images of the stained cells were obtained using an INCell Analyzer 2200 Imaging System (GE Healthcare Life Sciences) and processed using the

ImageJ software. 10 random fields were acquired per condition using a magnification of 20x. Image analysis and quantification was performed on *CellProfiler, a* cell image analysis software developed by the BROAD Institute. The number of DAPI-positive nuclei (total number of cells) and the number of TUNEL-positive nuclei were automatically counted, and the results presented as percentage of apoptotic nuclei of all DAPI-positive nuclei.

Glucose and lactate analyses

Glucose and lactate levels in the cell culture medium were analysed at the Core Biochemical Assay Laboratory, Clinical Biochemistry, Addenbrooke's Hospital using automated assays on a Siemens Dimension RxL analyser. The rate of glucose and lactate net change relative to cells over time (μmol/10^6 cells/24h) was calculated by subtracting the value measured at the end of the experiment (T=24h) from the one measured in a sample of medium collected at the onset of the incubation, and dividing the resulting value by the amount of cells in each experiment, multiplied by the experimental volume (2 ml). For oligodendrocyte cultures, the cell number considered was the cell number at plating since these cells do not proliferate. For astrocyte cultures (which proliferate to some extent), the cell number considered was determined at the end of the experiment, after collection of cells from two sample wells using trypsin-EDTA.

High performance liquid chromatography (HPLC)

HPLC was used to quantify the total amounts of amino acids in samples of cell extracts and medium. Samples were lyophilized and resuspended in 0.01M HCl and subsequently derivatized with *o*-phtaldialdehyde (Geddes and Wood 1984) using an automated method prior to injection into the HPLC column. The amino acid components were separated with a ZORBAX SB-C18 (4.6 × 150 mm, 3.55 micron) column from Agilent Technologies (Palo Alto, CA). As eluents, a mixture of 50 mM sodium phosphate buffer (pH 5.9) with 2.5%

tetrahydrofurane and a mixture of methanol (98.75%) with tetrahydrofurane (1.25%) were used. The samples were analyzed using a Hewlett Packard 1100 System (Agilent Technologies, Palo Alto, CA) with fluorescence detection. Amino acid concentrations were determined by comparison to a calibration curve of standard solutions of amino acids run after every 12 samples (Amaral et al. 2014).

Gas Chromatography-Mass Spectrometry (GC-MS)

For analysis of percent enrichment of ^{13}C in lactate, amino acids (alanine, aspartate, glutamate and glutamine) and TCA cycle intermediates (citrate and malate) after incubation with different ^{13}C labelled substrates, cell extracts and samples of medium were lyophilized and resuspended in 0.01M HCl. To move the metabolites of interest into the organic phase in their acid form, the pH was adjusted to pH<2 with 6 M HCl. Samples were dried under atmospheric air (50 °C), and metabolites were derivatised with MTBSTFA in the presence of 1% *t*-BDMS-Cl (Mawhinney et al. 1986). The protocol used for analysis of the glycolytic intermediates phosphoenolpyruvate (PEP) and 3-phosphoglycerate (3PG) was based on the protocol reported by Hofmann et al. (2008). Derivatization was performed using a mixture of MSTFA + 1% trimethylchlorosilane (TMS) and acetonitrile. The samples were analyzed on an Agilent 6890 gas chromatograph connected to an Agilent 5975B mass spectrometer (Agilent Technologies, Palo Alto, CA). The parent ion (M) and atom percent excess for one ^{13}C atom (M+1) values for 3PG, PEP, alanine, aspartate, lactate, citrate and glutamate were calculated from the GC-MS data using the MassHunter software supplied by Agilent (Agilent Technologies, Palo Alto, CA) and correcting for the naturally abundant ^{13}C by using non-enriched standards (Biemann 1962).

^{13}C and ^{1}H Nuclear Magnetic Resonance (NMR) Spectroscopy

^{13}C NMR spectroscopy was used to identify the synthesis of particular labelled isotopologues from [1,2-^{13}C]glucose metabolism due to the ability of this technique to distinguish between

the different carbon positions that are labelled in one molecule. For example, ^{13}C NMR spectroscopy enabled to distinguish between the presence of [2,3-^{13}C]glutamate (synthesized via pyruvate carboxylation) and [1,2-^{13}C]glutamate (synthesized via PDH; see below for further details). On the other hand, GC-MS is a more sensitive method that provides information about ^{13}C enrichment above natural abundance but lacks the specificity of NMR spectroscopy, as it does not provide information about the location of the ^{13}C label. GC-MS, as applied in the present study, only enables to distinguish between species that have a different number of ^{13}C labelled carbons. All NMR samples were analysed using a QCI CryoProbe™ 600MHz (for proton) ultrashielded Plus magnet (Bruker BioSpin GmbH, Reinstetten, Germany). ^{1}H NMR spectra were acquired using a pulse angle of 90°, 12 kHz spectral width with 66 data points, acquisition time of 2.66 seconds, relaxation delay of 10 seconds and 128 scans. These spectra were used to quantify the amount of glutamate for correction of natural abundance of [4-^{13}C]glutamate (to be used in the calculation of contribution of the PPP to [4-^{13}C]glutamate synthesis). Proton decoupled ^{13}C NMR spectra were obtained on the same instrument using a 30° pulse angle and 30 kHz spectral width with 98 000 data points employing an acquisition time of 1.65 seconds and a relaxation delay of 0.5 seconds. The number of scans needed to obtain an appropriate signal to noise ratio was 210 000. TopSpin™ 3.0 software (Bruker BioSpin GmbH, Reinstetten, Germany) was used for acquisition, integration, and quantification. Relevant peaks in the spectra were assigned and quantified from the integrals of the peaks using ethylene glycol as an internal standard with known amount of ^{13}C. Corrections for natural abundance as well as nuclear Overhauser enhancement and relaxation effects, relative to the internal standard, were applied to all relevant integrals from ^{13}C spectra.

Statistical analysis

Statistical analysis was conducted using unpaired two-tailed Student *t*-tests (confidence interval=95%).

Results

Characterisation of late differentiation-stage oligodendrocyte lineage cells *in vitro*

To study metabolic reactions in mature oligodendroglia cultures, highly enriched primary rat OPCs (Figure 1A) were differentiated in Sato's differentiation medium. At 5 days of differentiation the cells displayed the characteristically branched morphology of late oligodendrocyte lineage cells with approximately 65% of the cells expressing MBP (Figure 1B). To investigate the relative activity of different metabolic pathways in mature oligodendrocytes, cells were incubated with one of the following ^{13}C-labelled substrates: [1,6-^{13}C]glucose, [1,2-^{13}C]glucose, [1-^{13}C]lactate or [1,2-^{13}C]acetate.

Differentiated oligodendrocyte lineage cells display a significant activity of the pentose phosphate pathway

To investigate the relative activity of the glycolytic pathway versus the PPP, [1,2-^{13}C]glucose was added to the medium (Brekke et al. 2014; Dusick et al. 2007). Following 24h of incubation, cell extracts were collected and analysed using GC-MS and ^{13}C and ^{1}H NMR spectroscopy. If [1,2-^{13}C]glucose is metabolised via the glycolytic pathway, [2,3-^{13}C]3PG, [2,3-^{13}C]PEP and [2,3-^{13}C]pyruvate are formed (Figure 2A). [2,3-^{13}C]pyruvate can enter the mitochondria to be converted into [1,2-^{13}C]acetyl CoA. Condensation of [1,2-^{13}C]acetyl CoA with unlabelled oxaloacetate leads to the formation of the TCA cycle intermediate [1,2-^{13}C]citrate and then, following several steps, α-[4,5-^{13}C]ketoglutarate, which is subsequently converted into [4,5-^{13}C]glutamate. [1,2-^{13}C]glucose metabolism via the PPP gives rise to [3-^{13}C]3PG, [3-^{13}C]PEP, [3-^{13}C]pyruvate and [2-^{13}C]acetyl CoA (Figure 2B). [2-^{13}C]acetyl CoA can then be converted into [4-^{13}C]glutamate via the TCA cycle (Figure 2B).

Because PEP and 3PG are localized downstream of the intersection between glycolysis and the PPP, their ^{13}C isotopologues can be used to calculate the ratio between

glycolysis and the PPP. Analysis of PEP and 3PG enables detection of isotopologues that derive from the re-entry of metabolic intermediates (fructose-6P and GA3P) into glycolysis from the PPP. The intermediates of the PPP lose the ^{13}C in the C1 position via decarboxylation of [1,2-^{13}C]gluconate-6-phosphate by 6-phosphogluconate dehydrogenase and 1/3 of the molecules will re-enter glycolysis with only one labelled (M+1) carbon instead of two (M+2) – see Figure 2 and (Brekke et al. 2012) for further details. Based on GC-MS results, the M+2/M+1 ratios of PEP and 3PG were calculated, indicating that 10-15% of glucose is metabolised via the PPP in mature oligodendrocytes (Figure 2C). Of note, this ratio is likely to under-estimate the contribution of the PPP (for details see Brekke et al. 2012).

An alternative way to investigate the relative contribution of glycolysis and PPP to glucose metabolism is to apply ^{13}C NMR spectroscopy to differentiate between [4,5-^{13}C] and [4-^{13}C]glutamate (Figure 2D). In the ^{13}C NMR spectrum glycolysis-derived [4,5-^{13}C]glutamate is represented as a doublet in the C-4 region of glutamate (34.5 ppm), whereas PPP-derived [4-^{13}C]glutamate is represented as a singlet. The contribution of glucose metabolized via the PPP relative to glucose metabolized via glycolysis to the total glutamate synthesis was calculated by dividing the area of the [4-^{13}C]glutamate peak (after correction for natural abundance using ^{1}H NMR spectroscopy) by the area of the doublet peak [4,5-^{13}C]glutamate. We found that 10% ± 0.2% (mean ± s.e.m.; n=3) of the total glutamate comes from glucose metabolized in the PPP. Our results confirm that the PPP is active in oligodendrocytes and that it contributes to glutamate synthesis.

Evidence for PDH and mitochondrial activity in oligodendrocytes

To investigate the extent of oxidative metabolism in oligodendrocytes, cells were incubated with ^{13}C-labelled glucose or [1,2-^{13}C]acetate for 24h (for labelling patterns see Figure 3A, B). We confirmed that after 24h, all [1,6-^{13}C]glucose-derived metabolites, except for glutamine,

reached a steady-state of labelling (Supplementary Figure 1). Hence, we decided to investigate labelling patterns in cell lysates after 24 in all subsequent experiments. Assessing cell viability using TUNEL staining showed no differences between the various experimental conditions (Figure 3C). Metabolism of [1,6-^{13}C]glucose yields two molecules of [3-^{13}C]alanine and [3-^{13}C]pyruvate. The latter is then converted into [2-^{13}C]acetyl CoA, which can condense with non-labelled oxaloacetate to form mono-labelled (M+1) compounds in the first turn of the TCA cycle (described in Figure 3A). [2-^{13}C]acetyl CoA can also condense with labelled oxaloacetate and give rise to the formation of double-labelled (M+2) compounds in a combination of the first and second turn of the cycle (Figure 3A). GC-MS analysis of cell extracts incubated with [1,6-^{13}C]glucose (Figure 3D), showed that mitochondrial metabolism was prominent in mature oligodendrocytes. TCA cycle intermediates and amino acids were highly enriched ranging from 15-25% in citrate, malate, glutamate and glutamine and 10% in aspartate (Figure 3D). Moreover, a substantial enrichment was also observed with M+2 isotopologues and even M+3 (data not shown), typical of the second and third turns of the TCA cycle (see Figure 3D). However, the second turn of the TCA cycle is underestimated since labelled oxaloacetate can condense with unlabelled acetyl CoA and give rise to single labelled (M+1) compounds in the second turn. Second turn isotopologues were also observed when [1,2-^{13}C]glucose was used as substrate (Figure 3D). It is important to note that only half of the pyruvate molecules are labelled from [1,2-^{13}C]glucose and, therefore, the maximum enrichment levels will be half of those obtained from [1,6-^{13}C]glucose. Alanine is obtained from pyruvate transamination and is generally considered to be a metabolite related to glycolysis. The expected isotopologue of [1,2-^{13}C]glucose is [1,2-^{13}C]alanine. However, we observed M+1 alanine in addition to M+2 labelled alanine (Figure 3D). This is evidence for the presence of partial pyruvate recycling,

which can be performed via decarboxylation of malate or oxaloacetate into pyruvate (Sonnewald 2014).

Acetate metabolism in oligodendrocytes

Conversion of acetate into acetyl CoA is known to take place in astrocytes, but not in neurons (Sonnewald and Rae 2010). To investigate whether oligodendrocytes are able to convert acetate into acetyl CoA and oxidize it in the TCA cycle, cells were incubated with [1,2-^{13}C]acetate for 24h and the extra- and intracellular metabolites were analysed by GC-MS (Figure 3B, D). Both [1,2-^{13}C]acetate and [1,2-^{13}C]glucose identically yield [1,2-^{13}C]acetyl CoA (Figure 3B). Overall, the extent of labelling from [1,2-^{13}C]acetate was much lower than that from [1,2-^{13}C]glucose. Enrichment of the most abundant metabolites citrate and glutamate from [1,2-^{13}C]acetate was approximately half of enrichment obtained from [1,2-^{13}C]glucose; the less abundant metabolites aspartate and glutamine were poorly enriched. The abundance of M+1 isotopologues (typical of the second turn of the TCA cycle) derived from [1,2-^{13}C]acetate was very low (Figure 3D), suggesting that acetate-derived acetyl CoA is metabolised in a different compartment than pyruvate-derived acetyl CoA. Alanine enrichment from [1,2-^{13}C]acetate (albeit at low levels), confirms that oligodendrocytes have active partial pyruvate recycling, as observed in cells incubated with [1,2-^{13}C]glucose. In the medium, labelling from [1,2-^{13}C]acetate was only detectable in citrate, in which M+2 amounted to 10 ± 2% (mean ± s.e.m., n=12).

Glucose consumption and release of metabolites to the culture medium

Analysis of glucose consumption and lactate release rates (Figure 3E-I,II) indicates that oligodendrocytes metabolise glucose to an extent comparable to astrocytes (3.2±0.06 µmol/10^6 cells/24h; mean ± s.e.m.; n=6). However, oligodendrocytes release less lactate than

astrocytes (5.3 ± 0.16 μmol/10^6 cells/24h; mean ± s.e.m.; n=6). Although glucose consumption in the presence of 4 mM [1-^{13}C]lactate (Figure 3E-I) was increased, the net release of total lactate remained unchanged (Figure 3E-II). Due to the presence of [1-^{13}C]lactate in the culture medium, it was possible to distinguish between the uptake of [1-^{13}C]lactate and the release of endogenous (unlabelled) lactate (Figure 3E-III). This analysis showed that the presence of lactate in the medium increased the release of endogenous lactate (Figure 3E-III). The release of unlabelled lactate was at least 3-fold larger than the amount of [1-^{13}C]lactate consumed. By comparing lactate release rates and glucose consumption rates it was possible to estimate the fraction of glucose metabolized to lactate, versus the oxidation of pyruvate in the mitochondria. In oligodendrocytes cultured with glucose alone, the ratio of lactate production to pyruvate oxidation was 60:40 (and 80:20 in astrocytes). In the presence of lactate, the ratio changed to 30:70, indicating increased mitochondrial activity. Figure 3C shows that the viability of cells was not affected by the presence of lactate.

Despite the substantial % enrichment of ^{13}C in the above-mentioned amino acids observed in the cell extracts, only negligible release of alanine and glutamine was detected (data not shown).

Pyruvate carboxylation in oligodendrocytes

Pyruvate carboxylation is an important anaplerotic pathway known to operate in astrocytes but not in neurons (McKenna et al. 2012). The presence of this pathway was probed in mature oligodendrocytes by using either [1,2-^{13}C]glucose or [1-^{13}C]lactate (Figure 4). [1-^{13}C]lactate is a valuable substrate for this purpose since only via pyruvate carboxylation the ^{13}C label from [1-^{13}C]lactate can be found in the TCA cycle intermediate citrate (PDH removes carbon number 1 from pyruvate generating unlabelled acetyl CoA, and therefore the ^{13}C label is lost via PDH; Figure 4A). In order to evaluate the significance of pyruvate carboxylation in

oligodendrocytes, also astrocytes (the cells known to carboxylate pyruvate in the brain) were incubated with [1-^{13}C]lactate. Both of these cell types were shown to oxidize lactate to a large extent in culture (Sanchez-Abarca et al. 2001). [1-^{13}C]Pyruvate carboxylation was apparent in the labelling of citrate in the medium in both cell types (Figure 4B). However, in the cell extracts this was only evident in astrocytes. A possible explanation for the absence of intracellular citrate enrichment in oligodendrocytes is a potential compartmentation of pyruvate metabolism, which has also been shown for astrocytes and neurons (Bak et al. 2007; Bakken et al. 1997).

To further investigate the presence of pyruvate carboxylation, oligodendrocytes were also incubated with medium containing [1,2-^{13}C]glucose. The C-2 region of glutamate (around 55.5 ppm) in the ^{13}C NMR spectrum of cell extracts was analysed to confirm the presence of pyruvate carboxylation (Figure 4C). From the scheme depicted in Figure 4C it emerges that only pyruvate carboxylation will lead to the formation of [2,3-^{13}C]glutamate whereas [1,2-^{13}C]glutamate (and [3-^{13}C]glutamate, which is not shown) is formed from pyruvate dehydrogenation (and pyruvate carboxylation, if the label stays in the cycle for an additional turn). The spectrum shown in Figure 4C, which reflects the presence of [2,3-^{13}C]glutamate, indicates that oligodendrocytes carboxylate pyruvate.

Discussion

Although oligodendrocytes make up a significant proportion of brain cells, their metabolic properties remain largely unknown. In a recent review we have called for a systematic study of metabolic pathways in oligodendrocytes (Amaral et al. 2013). In the present work, we study aspects of glucose, lactate, and acetate metabolism in oligodendrocytes, and specifically address the activity of the PPP and whether oligodendrocytes are able to conduct anaplerotic and cataplerotic reactions based on carboxylation of pyruvate and decarboxylation of malate or oxaloacetate.

Primary rat OPCs were purified from perinatal rat mixed glial cultures (McCarthy and de Vellis 1980). This approach results in high yields of relatively pure (>93%) cultures. Culture of the O4+, A2B5+, O1-, CNP-, MBP- OPCs in Sato's medium triggers a highly predictable series of morphological and transcriptional events and results in the formation of mature oligodendrocytes with complex branched processes and membrane sheets, which express late stage markers, including MBP. Although a significant proportion of cells (approximately 60%) reach a mature oligodendrocyte stage, the cultures also include late stage progenitors. Genomic studies comparing acutely isolated cells at distinct developmental stages with the culture system used in the present study confirmed that primary OPC cultures faithfully represent their *in vivo* counterparts (Dugas et al. 2006).

Our results demonstrate that oligodendrocytes have extensive glucose-derived metabolism. In fact, we found that the rate of glucose consumption in oligodendrocytes is comparable to the one in astrocytes. Although Sanchez-Abarca et al (2001) previously concluded that oligodendrocytes utilize more glucose than astrocytes, they also showed that oligodendrocytes metabolise a larger proportion of glucose via PDH than astrocytes. We obtained a similar result by comparing the ratios of lactate release to glucose consumption in both cell types. Furthermore, we observed that both glucose consumption and the proportion

of glucose-derived pyruvate metabolised in the mitochondria were increased in the presence of exogenous lactate. This suggests that lactate may act as metabolic activator in oligodendrocytes, fitting with the concept that lactate can act as signalling molecule (Rinholm and Bergersen 2014). Furthermore, our results confirm that oligodendrocytes are able to release substantial amounts of lactate *in vitro* as has been reported *in vivo* by Funfschilling et al. (2012). Also, it is possible that, at least, a proportion of the [1-^{13}C]lactate taken up was oxidized for lipogenesis, as proposed by (Sanchez-Abarca et al. 2001). In spite of the presence of 4 mM exogenous lactate, a net production of lactate was observed indicating that glycolysis in oligodendrocytes is not inhibited by extracellular lactate.

The PPP is a glucose shunt, which is thought to be active in neurons and astrocytes (Almeida et al. 2002; Amaral et al. 2010; Bolanos and Almeida 2010; Brekke et al. 2012; Garcia-Nogales et al. 2003). Using ^{14}C tracing techniques (Edmond et al. 1987) showed active PPP in oligodendrocyte lineage cells. Sanchez-Abarca et al. (2001) reported PPP activity in immature OPC cultures as being 2-fold higher than in astrocytes and 4-fold higher than in neurons. Our approach measured the contribution of the PPP to the synthesis of glycolytic intermediates and glutamate synthesis based on ^{13}C-tracing techniques. In our study, the labelling of the glycolytic intermediates PEP and 3PG indicate that mature oligodendrocytes use approximately 10-15% of glucose in the PPP compared to glycolysis. These values are in the range of previously published data for cortical astrocyte cultures in a metabolic modelling study also using ^{13}C-labelled substrates (Amaral et al. 2011a), which contrasts with the report by Sanchez-Abarca et al (2001). It is possible that our cultures contain more mature oligodendrocytes than those used by Sanchez-Abarca et al., and therefore have a lower PPP activity, more closely resembling the rate in astrocytes. On the basis of ^{14}C tracing experiments, Sykes et al. reported that, although the PPP oxidizes only <3% of the glucose consumed, it produces more CO_2 than the TCA cycle in primary

oligodendrocyte lineage cells, due to its close link to de novo synthesis of fatty acids and cholesterol (Sykes et al. 1986). Since we did not measure the contribution of glucose to lipid synthesis, it is possible that our approach underestimated the total use of glucose via the PPP.

For the first time, our experiments demonstrate that pyruvate generated from glucose via the PPP contributes to the synthesis of acetyl CoA for oxidation and generation of metabolites in the TCA cycle in oligodendrocytes. We found that approximately 10% of the glutamate produced derives from glucose metabolized in the PPP. Estimation of the PPP activity on the basis of glutamate isotopomers indicated that the PPP accounted for approximately 6% of glucose metabolism in cortical neurons and approximately 4% in cerebellar neurons (Brekke et al. 2012). Similar to reports in neurons (Brekke et al. 2012), we found that oligodendrocytes incorporate ^{13}C label in glutamate produced by [1,2-^{13}C]glucose metabolism via the PPP.

The PPP may also play a role in diseases that affect oligodendrocytes. E.g. increased activity of the transaldolase, an enzyme which forms part of the non-oxidative branch of the PPP and is involved in lipid and nucleotide synthesis, has been reported in oligodendrocytes in brains of MS patients, compared to healthy controls (Banki et al. 1994). NADPH produced in the PPP is fundamentally important for the synthesis of glutathione, which is thought to protect myelin sheaths from oxidative stress. Banki and colleagues proposed that auto-antibodies against transaldolase found in MS patients, may cause destruction of oligodendrocytes via depletion of transaldolase. Altered PPP activity was also reported in a study of patients that suffered a traumatic brain injury (TBI) (Dusick et al. 2007). It is possible that, at least, a proportion of the PPP alterations observed in the study by Dusick et al (2007) could be linked to the extensive demyelination that is thought to occur in TBI patients (Armstrong et al. 2015).

Using different forms of ^{13}C labelled glucose we demonstrate that our cultures also exhibit a high rate of mitochondrial metabolism, as previously suggested by Sanchez-Abarca et al. (2001). Whereas functional mitochondria seem to be important for OPC differentiation (Schoenfeld et al. 2010; Ziabreva et al. 2010), it was recently proposed that myelinating oligodendrocytes are not dependent on mitochondrial activity *in vivo* (Funfschilling et al. 2012). The most likely explanation for the discrepancy between the high mitochondrial demands of our cultures and the findings *in vivo* is the significant presence of pre-myelinating (MBP-negative) OPCs that have not yet reached fully mature stages *in vitro*. Our data thus may reflect the prominent role of oxidative metabolism at the late stages of OPC differentiation, including the pre-myelinating and early myelinating stages.

Another important question with respect to mitochondrial metabolism in oligodendrocytes is whether they can replenish TCA cycle intermediates via anaplerosis. It is well established that neurons depend on astrocytes for replenishing their TCA cycle intermediates. As neurons cannot carboxylate pyruvate, external TCA cycle intermediates are required for the synthesis of amino acid neurotransmitters (McKenna et al. 2012). Whether and to which extent oligodendrocytes are self-sufficient with respect to the production of anaplerotic substrates remained unknown. By incubating cells with [1,2-^{13}C]glucose we found that pyruvate carboxylation indeed takes place in oligodendrocytes as shown by the production of [2,3-^{13}C]glutamate. This was further confirmed by label incorporation in citrate in the medium of cells incubated with [1-^{13}C]lactate, which is only possible via pyruvate carboxylation. Comparable label incorporation from [1-^{13}C]lactate was found in citrate in the medium of astrocyte cultures. This suggests that lactate is metabolised in a similar way in the TCA cycle of both cell types. However, it is possible that a fraction of the lactate taken up by our cultures was used for lipogenesis (Sanchez-Abarca et al. 2001). It must also be noted that the overall contribution of pyruvate carboxylation to oligodendrocyte and astrocyte

metabolism is underestimated in the experiments based on [1-^{13}C]lactate metabolism because [1-^{13}C]pyruvate derived from [1-^{13}C]lactate competes with unlabelled pyruvate derived from glucose, which is also present in the incubation medium.

Pyruvate can be carboxylated to oxaloacetate by PC or to malate and NADP+ by malic enzyme. Whether PC or malic enzyme is responsible for pyruvate carboxylation in oligodendrocytes remains to be established. Murin et al. (2009) reported PC expression in cultured oligodendroglia. Whether oligodendrocytes express malic enzyme remains unknown. In neurons and astrocytes, malic enzyme only contributes to pyruvate production (McKenna et al. 2000; McKenna et al. 1995). However, PC is thought to be the most important anaplerotic enzyme in the brain (Patel 1974). Irrespective of which enzyme is responsible for pyruvate carboxylation, the detection of carboxylation (and thus anaplerosis) has consequences for oligodendrocyte metabolism. If oligodendrocytes (similarly to neurons) were not capable of anaplerosis they would depend on the provision of glutamine by astrocytes, which have a net production of glutamine via pyruvate carboxylation (Gamberino et al. 1997; Waagepetersen et al. 2001).

An alternative route to replenish the TCA cycle in oligodendrocytes is to use aspartate, liberated from N-acetyl aspartate (NAA), which in turn is supplied by neurons (Moffett et al. 2007). However, aspartate released by NAA hydrolysis in oligodendrocytes could potentially be sent back to neurons, thus avoiding the depletion of anaplerotic substrates in neurons (NAA synthesis in neurons is dependent on glutamine entry from astrocytes). Our results indicate that oligodendrocytes are capable of anaplerosis, which suggests that they are potentially independent of astrocytic pyruvate carboxylation. Whether the level of anaplerosis in oligodendrocytes is sufficient to meet their entire requirements is not known at present. It is also unclear whether aspartate is shuttled back to neurons or whether it is metabolized in

oligodendrocytes. Both possibilities have previously been suggested but evidence is lacking (Baslow and Guilfoyle 2006; Moffett et al. 2007).

Acetyl CoA is an essential molecule in the TCA cycle. Most acetyl CoA derives from pyruvate via PDH. However, oligodendrocytes are known to express the enzyme aspartoacylase, which catalyzes the hydrolysis of NAA into aspartate and acetate (Moffett et al. 2011). NAA-derived acetate significantly contributes to myelin lipid synthesis in the CNS (Chakraborty et al. 2001) and is also thought to support oxidative metabolism during myelination (Francis et al. 2012). Furthermore, oligodendrocytes express acetyl CoA synthetase-1, which catalyzes the synthesis of acetyl coenzyme A from acetate and coenzyme A, indicating that acetate may contribute to lipid synthesis, especially during postnatal brain development (Ariyannur et al. 2010). So far only astrocytes were shown to convert acetate into acetyl CoA whereas neurons do not seem able to do so (Muir et al. 1986; Sonnewald et al. 1993a). Consequently, acetate has been used extensively to assess astrocyte metabolism in the context of astrocytic-neuronal interactions *in vivo* (e.g. Melo et al. 2005; Morken et al. 2014; Nilsen et al. 2014), in neurospheres (Sa Santos et al. 2011) and in culture (Sonnewald et al. 1993a). However, potential metabolic contributions from oligodendrocytes were not considered in these studies. The present work demonstrates that mature oligodendrocyte cultures are able to convert acetate into acetyl CoA and oxidize it in the mitochondria as shown by the incorporation of ^{13}C label from [1,2-^{13}C]acetate into the TCA cycle intermediates malate and citrate and the amino acids glutamate and glutamine. Labelling from [1,2-^{13}C]acetate was not as pronounced as labelling from [1,2-^{13}C]glucose but, nevertheless, significant and comparable to that observed in astrocytes (data not shown). However, astrocytes label glutamine extensively from ^{13}C-labelled acetate (Hassel et al. 1995), whereas oligodendrocytes do not. Surprisingly, we found that alanine was also labelled from [1,2-^{13}C]acetate, and that alanine M+1 enrichment was detected in oligodendrocytes incubated

with [1,2-^{13}C]glucose. Both isotopologues of alanine could not have been produced without the participation of the TCA cycle and malic enzyme or pyruvate kinase (PK) and phosphoenolpyruvate carboxykinase (PEPCK) (Cruz et al. 1998). This indicates that pyruvate recycling, a catabolic pathway (Amaral et al. 2011b; Cerdan et al. 1990; Haberg et al. 1998; Kunnecke et al. 1993; Olstad et al. 2007), is not only active in astrocytes and neurons but also in oligodendrocytes.

Conclusion

Our results show that oligodendrocyte lineage cells at late stages of differentiation are metabolically active cells and have distinct metabolic properties. We found that the cells were able to conduct all the metabolic functions that were investigated and, therefore, demonstrate a high degree of cellular independence. Figure 5 summarizes the findings of the present series of experiments and integrates our data with the known pathways linking astroglial and neuronal metabolism. Our results indicate that metabolic functions of oligodendroglia need to be considered in studies investigating glucose metabolism in CNS tissue or whole brain studies. This work reinforces the emerging role of oligodendrocyte metabolism with respect to neuronal-glial interactions.

Acknowledgements

This work was supported by grants from the UK Multiple Sclerosis Society and from Qatar Foundation. We acknowledge the excellent technical support in GC-MS and HPLC analysis from Lars Evje (NTNU, Norway). We declare no conflict of interest related to this work.

References

Almeida A, Delgado-Esteban M, Bolanos JP, Medina JM. 2002. Oxygen and glucose deprivation induces mitochondrial dysfunction and oxidative stress in neurones but not in astrocytes in primary culture. J Neurochem 81:207-217.

Amaral AI, Meisingset TW, Kotter MR, Sonnewald U. 2013. Metabolic aspects of neuron-oligodendrocyte-astrocyte interactions. Front Endocrinol (Lausanne) 4:54.

Amaral AI, Teixeira AP, Haakonsen BI, Sonnewald U, Alves AM. 2011a. A comprehensive metabolic profile of cultured astrocytes using isotopic transient metabolic flux analysis and ^{13}C-labeled glucose. Front Neuroenerg 3:5.

Amaral AI, Teixeira AP, Martens S, Bernal V, Sousa MFQ, Alves PM. 2010. Metabolic alterations induced by ischemia in primary cultures of astrocytes: merging ^{13}C NMR spectroscopy and metabolic flux analysis. J Neurochem 113:735-748.

Amaral AI, Teixeira AP, Sonnewald U, Alves PM. 2011b. Estimation of intracellular fluxes in cerebellar neurons after hypoglycemia: importance of the pyruvate recycling pathway and glutamine oxidation. J Neurosci Res 89:700-10.

Amaral AI, Alves PM, Teixeira AP. 2014. Metabolic Fux Analysis Tools to Investigate Brain Metabolism In Vitro. In: Hirrlinger J, Waagepertersen, HS. , editor. Brain Energy Metabolism. New York: Humana Press. p 107-144.

Ariyannur PS, Moffett JR, Madhavarao CN, Arun P, Vishnu N, Jacobowitz DM, Hallows WC, Denu JM, Namboodiri AM. 2010. Nuclear-cytoplasmic localization of acetyl coenzyme a synthetase-1 in the rat brain. J Comp Neurol 518:2952-77.

Armstrong RC, Mierzwa AJ, Sullivan GM, Sanchez MA. 2015. Myelin and oligodendrocyte lineage cells in white matter pathology and plasticity after traumatic brain injury. Neuropharmacology doi: 10.1016/j.neuropharm.2015.04.029. [Epub ahead of print].

Attwell D, Laughlin SB. 2001. An energy budget for signaling in the grey matter of the brain. J Cereb Blood Flow Metab 21:1133-1145.

Baer AS, Syed YA, Kang SU, Mitteregger D, Vig R, Ffrench-Constant C, Franklin RJ, Altmann F, Lubec G, Kotter MR. 2009. Myelin-mediated inhibition of oligodendrocyte precursor differentiation can be overcome by pharmacological modulation of Fyn-RhoA and protein kinase C signalling. Brain 132:465-81.

Bak LK, Waagepetersen HS, Melo TM, Schousboe A, Sonnewald U. 2007. Complex glutamate labeling from [U-^{13}C]glucose or [U-^{13}C]lactate in co-cultures of cerebellar neurons and astrocytes. Neurochem Res 32:671-80.

Bakken IJ, White LR, Aasly J, Unsgard G, Sonnewald U. 1997. Lactate formation from [U-^{13}C]aspartate in cultured astrocytes: compartmentation of pyruvate metabolism. Neurosci Lett 237:117-120.

Banki K, Colombo E, Sia F, Halladay D, Mattson DH, Tatum AH, Massa PT, Phillips PE, Perl A. 1994. Oligodendrocyte-specific expression and autoantigenicity of transaldolase in multiple sclerosis. J Exp Med 180:1649-63.

Baslow MH, Guilfoyle DN. 2006. Functions of N-acetylaspartate and N-acetylaspartyl-glutamate in brain - Evidence of a role in maintenance of higher brain integrative activities of information processing and cognition. In: Moffett JR, Tieman SB, Weinberger DR, Coyle JT, Namboodiri AMA, editors. N-Acetylaspartate: A Unique Neuronal Molecule in the Central Nervous System. Bethesda, MD: Springer. p 95-112.

Biemann K. 1962. The mass spectra of isotopically labeled molecules. Mass spectrometry; Organic chemical applications. New York: McGraw-Hill. p 223-227.

Bolanos JP, Almeida A. 2010. The pentose-phosphate pathway in neuronal survival against nitrosative stress. IUBMB life 62:14-8.

Brekke EM, Morken TS, Wideroe M, Haberg AK, Brubakk AM, Sonnewald U. 2014. The pentose phosphate pathway and pyruvate carboxylation after neonatal hypoxic-ischemic brain injury. J Cereb Blood Flow Metab 34:724-34.

Brekke EM, Walls AB, Schousboe A, Waagepetersen HS, Sonnewald U. 2012. Quantitative importance of the pentose phosphate pathway determined by incorporation of ^{13}C from [2-13C]- and [3-13C]glucose into TCA cycle intermediates and neurotransmitter amino acids in functionally intact neurons. J Cereb Blood Flow Metab 32:1788-99.

Cerdan S, Kunnecke B, Seelig J. 1990. Cerebral metabolism of [1,2-$^{13}C_2$]acetate as detected by in vivo and in vitro ^{13}C NMR. J Biol Chem 265:12916-26.

Cesar M, Hamprecht B. 1995. Immunocytochemical examination of neural rat and mouse primary cultures using monoclonal antibodies raised against pyruvate carboxylase. J Neurochem 64:2312-2318.

Chakraborty G, Mekala P, Yahya D, Wu G, Ledeen RW. 2001. Intraneuronal N-acetylaspartate supplies acetyl groups for myelin lipid synthesis: evidence for myelin-associated aspartoacylase. J Neurochem 78:736-45.

Cruz F, Scott SR, Barroso I, Santisteban P, Cerdan S. 1998. Ontogeny and cellular localization of the pyruvate recycling system in rat brain. J Neurochem 70:2613-9.

Dugas JC, Tai YC, Speed TP, Ngai J, Barres BA. 2006. Functional genomic analysis of oligodendrocyte differentiation. J Neurosci 26:10967-83.

Dusick JR, Glenn TC, Lee WN, Vespa PM, Kelly DF, Lee SM, Hovda DA, Martin NA. 2007. Increased pentose phosphate pathway flux after clinical traumatic brain injury: a [1,2-$^{13}C_2$]glucose labeling study in humans. J Cereb Blood Flow Metab 27:1593-602.

Edmond J, Robbins RA, Bergstrom JD, Cole RA, de Vellis J. 1987. Capacity for substrate utilization in oxidative metabolism by neurons, astrocytes, and oligodendrocytes from developing brain in primary culture. J Neurosci Res 18:551-61.

Francis JS, Strande L, Markov V, Leone P. 2012. Aspartoacylase supports oxidative energy metabolism during myelination. J Cereb Blood Flow Metab 32:1725-36.

Funfschilling U, Supplie LM, Mahad D, Boretius S, Saab AS, Edgar J, Brinkmann BG, Kassmann CM, Tzvetanova ID, Mobius W and others. 2012. Glycolytic oligodendrocytes maintain myelin and long-term axonal integrity. Nature 485:517-21.

Gamberino WC, Berkich DA, Lynch CJ, Xu B, LaNoue KF. 1997. Role of pyruvate carboxylase in facilitation of synthesis of glutamate and glutamine in cultured astrocytes. J Neurochem 69:2312-2325.

Garcia-Nogales P, Almeida A, Bolanos JP. 2003. Peroxynitrite protects neurons against nitric oxide-mediated apoptosis. A key role for glucose-6-phosphate dehydrogenase activity in neuroprotection. J Biol Chem 278:864-74.

Geddes JW, Wood JD. 1984. Changes in the amino acid content of nerve endings (synaptosomes) induced by drugs that alter the metabolism of glutamate and gamma-aminobutyric acid. J Neurochem 42:16-24.

Gegelashvili G, Schousboe A. 1997. High affinity glutamate transporters: regulation of expression and activity. Mol Pharmacol 52:6-15.

Gegelashvili G, Schousboe A. 1998. Cellular distribution and kinetic properties of high-affinity glutamate transporters. Brain Res Bull 45:233-238.

Haberg A, Qu H, Bakken IJ, Sande LM, White LR, Haraldseth O, Unsgard G, Aasly J, Sonnewald U. 1998. In vitro and ex vivo ^{13}C-NMR spectroscopy studies of pyruvate recycling in brain. Dev Neurosci 20:389-98.

Hassel B, Sonnewald U, Fonnum F. 1995. Glial-neuronal interactions as studied by cerebral metabolism of [2-^{13}C]acetate and [1-^{13}C]glucose: an ex vivo ^{13}C NMR spectroscopic study. J Neurochem 64:2773-82.

Hertz L, Yu A, Svenneby G, Kvamme E, Fosmark H, Schousboe A. 1980. Absence of preferential glutamine uptake into neurons--an indication of a net transfer of TCA constituents from nerve endings to astrocytes? Neurosci Lett 16:103-109.

Hofmann U, Maier K, Niebel A, Vacun G, Reuss M, Mauch K. 2008. Identification of metabolic fluxes in hepatic cells from transient 13C-labeling experiments: Part I. Experimental observations. Biotechnol Bioeng 100:344-54.

Kostic M, Zivkovic N, Stojanovic I. 2013. Multiple sclerosis and glutamate excitotoxicity. Rev Neurosci 24:71-88.

Kunnecke B, Cerdan S, Seelig J. 1993. Cerebral metabolism of [1,2-$^{13}C_2$]glucose and [U-$^{13}C_4$]3-hydroxybutyrate in rat brain as detected by ^{13}C NMR spectroscopy. NMR Biomed 6:264-277.

Lee Y, Morrison BM, Li Y, Lengacher S, Farah MH, Hoffman PN, Liu Y, Tsingalia A, Jin L, Zhang PW and others. 2012. Oligodendroglia metabolically support axons and contribute to neurodegeneration. Nature 26:443-8.

Lyons SA, Kettenmann H. 1998. Oligodendrocytes and microglia are selectively vulnerable to combined hypoxia and hypoglycemia injury in vitro. J Cereb Blood Flow Metab 18:521-30.

Martinez-Hernandez A, Bell KP, Norenberg MD. 1977. Glutamine synthetase: glial localization in brain. Science 195:1356-1358.

Mawhinney TP, Robinett RS, Atalay A, Madson MA. 1986. Analysis of amino acids as their tert.-butyldimethylsilyl derivatives by gas-liquid chromatography and mass spectrometry. J Chromatogr 358:231-242.

McCarthy KD, de Vellis J. 1980. Preparation of separate astroglial and oligodendroglial cell cultures from rat cerebral tissue. J Cell Biol 85:890-902.

McKenna M, Gruetter R, Sonnewald U, Waagepetersen HS, Schousboe A. S. 2012. Energy Metabolism of the Brain. In: Brady S. T. SGJ, Albers R. W., Price D. L., editor. Basic Neurochemistry: Principles of Molecular, Cellular, and Medical Neurobiology, 8th Edition,. Oxford, UK: Elsevier Academic Press. p 200-231.

McKenna MC, Stevenson JH, Huang X, Tildon JT, Zielke CL, Hopkins IB. 2000. Mitochondrial malic enzyme activity is much higher in mitochondria from cortical synaptic terminals compared with mitochondria from primary cultures of cortical neurons or cerebellar granule cells. Neurochem Int 36:451-9.

McKenna MC, Tildon JT, Stevenson JH, Huang X, Kingwell KG. 1995. Regulation of mitochondrial and cytosolic malic enzymes from cultured rat brain astrocytes. Neurochem Res 20:1491-501.

Melo TM, Nehlig A, Sonnewald U. 2005. Metabolism is normal in astrocytes in chronically epileptic rats: a ^{13}C NMR study of neuronal-glial interactions in a model of temporal lobe epilepsy. J Cereb Blood Flow Metab 25:1254-64.

Mifsud G, Zammit C, Muscat R, Di Giovanni G, Valentino M. 2014. Oligodendrocyte pathophysiology and treatment strategies in cerebral ischemia. CNS Neurosci Ther 20:603-12.

Moffett JR, Arun P, Ariyannur PS, Garbern JY, Jacobowitz DM, Namboodiri AM. 2011. Extensive aspartoacylase expression in the rat central nervous system. Glia 59:1414-34.

Moffett JR, Ross B, Arun P, Madhavarao CN, Namboodiri AM. 2007. N-Acetylaspartate in the CNS: from neurodiagnostics to neurobiology. Prog Neurobiol 81:89-131.

Morken TS, Brekke E, Haberg A, Wideroe M, Brubakk AM, Sonnewald U. 2014. Altered Astrocyte-Neuronal Interactions After Hypoxia-Ischemia in the Neonatal Brain in Female and Male Rats. Stroke 45:2777-85.

Muir D, Berl S, Clarke DD. 1986. Acetate and fluoroacetate as possible markers for glial metabolism in vivo. Brain Res 380:336-40.

Murin R, Cesar M, Kowtharapu BS, Verleysdonk S, Hamprecht B. 2009. Expression of pyruvate carboxylase in cultured oligodendroglial, microglial and ependymal cells. Neurochem Res 34:480-9.

Nilsen LH, Witter MP, Sonnewald U. 2014. Neuronal and astrocytic metabolism in a transgenic rat model of Alzheimer's disease. J Cereb Blood Flow Metab 34:906-14.

Norenberg MD, Martinez-Hernandez A. 1979. Fine structural localization of glutamine synthetase in astrocytes of rat brain. Brain Res 161:303-10.

Olstad E, Olsen GM, Qu H, Sonnewald U. 2007. Pyruvate recycling in cultured neurons from cerebellum. J Neurosci Res 85:3318-25.

Patel MS. 1974. The relative significance of CO_2-fixing enzymes in the metabolism of rat brain. J Neurochem 22:717-24.

Pitt D, Werner P, Raine CS. 2000. Glutamate excitotoxicity in a model of multiple sclerosis. Nat Med 6:67-70.

Reubi JC, van den Berg C, Cuenod M. 1978. Glutamine as precursor for the GABA and glutamate trasmitter pools. Neurosci Lett 10:171-4.

Rinholm JE, Bergersen LH. 2014. White matter lactate--does it matter? Neuroscience 276:109-16.

Sa Santos S, Sonnewald U, Carrondo MJ, Alves PM. 2011. The role of glia in neuronal recovery following anoxia: In vitro evidence of neuronal adaptation. Neurochem Int 58:665-75.

Sanchez-Abarca LI, Tabernero A, Medina JM. 2001. Oligodendrocytes use lactate as a source of energy and as a precursor of lipids. Glia 36:321-9.

Schoenfeld R, Wong A, Silva J, Li M, Itoh A, Horiuchi M, Itoh T, Pleasure D, Cortopassi G. 2010. Oligodendroglial differentiation induces mitochondrial genes and inhibition of mitochondrial function represses oligodendroglial differentiation. Mitochondrion 10:143-50.

Shank RP, Bennett GS, Freytag SO, Campbell GL. 1985. Pyruvate carboxylase: an astrocyte-specific enzyme implicated in the replenishment of amino acid neurotransmitter pools. Brain Res 329:364-7.

Simonishvili S, Jain MR, Li H, Levison SW, Wood TL. 2013. Identification of Bax-interacting proteins in oligodendrocyte progenitors during glutamate excitotoxicity and perinatal hypoxia-ischemia. ASN Neuro 23;5(5):e00131.

Sonnewald U. 2014. Glutamate synthesis has to be matched by its degradation - where do all the carbons go? J Neurochem 131:399-406.

Sonnewald U, Rae C. 2010. Pyruvate Carboxylation in Different Model Systems Studied by ^{13}C MRS. Neurochem Res 35:1916-21.

Sonnewald U, Westergaard N, Hassel B, Muller TB, Unsgard G, Fonnum F, Hertz L, Schousboe A, Petersen SB. 1993a. NMR spectroscopic studies of ^{13}C acetate and ^{13}C glucose metabolism in neocortical astrocytes: evidence for mitochondrial heterogeneity. Dev Neurosci 15:351-8.

Sonnewald U, Westergaard N, Schousboe A, Svendsen JS, Unsgard G, Petersen SB. 1993b. Direct Demonstration by ^{13}C NMR Spectroscopy That Glutamine from Astrocytes Is a Precursor for Gaba Synthesis in Neurons. Neurochem Int 22:19-29.

Sykes JE, Lopes-Cardozo M, Van Den Bergh SG. 1986. Relationship between the pentose-phosphate pathway and the de novo synthesis of fatty acids and cholesterol in oligodendrocyte-enriched glial cultures. Neurochem Int 8:77-82.

van den Berg CJ, Garfinkel D. 1971. A stimulation study of brain compartments. Metabolism of glutamate and related substances in mouse brain. Biochem J 123:211-218.

Waagepetersen HS, Sonnewald U, Larsson OM, Schousboe A. 2001. Multiple compartments with different metabolic characteristics are involved in biosynthesis of intracellular and released glutamine and citrate in astrocytes. Glia 35:246-252.

Yan H, Rivkees SA. 2006. Hypoglycemia influences oligodendrocyte development and myelin formation. Neuroreport 17:55-9.

Ziabreva I, Campbell G, Rist J, Zambonin J, Rorbach J, Wydro MM, Lassmann H, Franklin RJ, Mahad D. 2010. Injury and differentiation following inhibition of mitochondrial respiratory chain complex IV in rat oligodendrocytes. Glia 58:1827-37.

Figure legends

Figure 1 - Purity of the primary cultures of rat oligodendrocytes. Oligodendrocyte precursor cells were isolated from mixed glia cultures and cultured in Sato's medium + 0.05% FCS to induce differentiation. At day 1 of differentiation, more than 93% of the cells expressed the oligodendroglial lineage marker O4 (A) and at 5 days of differentiation approximately 65% of the cells expressed myelin basic protein (MBP), a marker of mature oligodendrocytes (B). Scale bars, 50 µm.

Figure 2 - Evidence of PPP activity in mature oligodendrocytes in culture after incubation with [1,2-^{13}C]glucose. Labelling patterns derived from [1,2-^{13}C]glucose metabolism via glycolysis (A) and the pentose phosphate pathway (PPP) (B). The % enrichment of ^{13}C in M+1 and M+2 isotopologues for 3PG and PEP was determined using GC-MS analysis of cell extracts after 24h incubation with [1,2-^{13}C]glucose. The ratio shown in (C) between M+1 (labelling from the PPP) and M+2 (labelling from glycolysis) enables to estimate the contribution of the PPP versus glycolysis to the formation of the glycolytic intermediates 3PG and PEP in mature oligodendrocyte (mean ± s.e.m.; n=3). (D) ^{13}C nuclear magnetic resonance spectrum of a cell extract from cultures incubated in medium containing [1,2-^{13}C]glucose for 24 h. The C-4 region of glutamate at 34.5 ppm (GLU) is shown. The doublet peak represents [4,5-^{13}C]glutamate ([4,5-^{13}C]GLU) which derives from glucose metabolism via glycolysis only. The singlet peak corresponds to [4-^{13}C]glutamate ([4-^{13}C]GLU) which is produced after glucose metabolism via the PPP. Abbreviations: 3PG, 3-phosphoglycerate; GLU, glutamate; PEP, phosphoenolpyruvate; PDH, pyruvate dehydrogenase; M+1, parent ion with one ^{13}C atom; M+2, parent ion with two ^{13}C atoms.

Figure 3. Evidence of high TCA cycle activity and acetate metabolism in mature oligodendrocytes in culture. Oligodendrocytes were differentiated for 5 days and incubated for 24h in medium containing [1,6-^{13}C]glucose (A), [1,2-^{13}C]glucose (B), or [1,2-^{13}C]acetate (B), followed by GC-MS analysis of samples of cell culture medium and cell extracts. A and B describe the labelling patterns deriving from the metabolism of these ^{13}C-labelled substrates. The isotopologues formed in the second turn of the TCA cycle result from condensation of labelled oxaloacetate (OAA) with labelled or unlabelled acetyl CoA. (C) Quantification of TUNEL positive/total cell number (given by DAPI staining) in cells incubated with glucose alone (mean ± s.e.m., n=12), glucose and lactate (mean ± s.e.m., n=10) or acetate (mean ± s.e.m., n=8); (D) % enrichment of ^{13}C in intracellular alanine and TCA cycle-related metabolites derived from each of the substrates (mean ± s.e.m., n=8 for [1,6-^{13}C]glucose, mean ± s.e.m., n=6 for [1,2-^{13}C]glucose and mean ± s.e.m., n=12 for [1,2-^{13}C]acetate). (E) Glucose (I) and lactate (II) net change in the medium in experiments performed in the presence of glucose alone or glucose + [1-^{13}C]lactate. For the experiment where [1-^{13}C]lactate was used, the net change of ^{13}C-labelled and unlabelled lactate is shown (III) (mean ± s.e.m., n=9). # - significantly different from the glucose + [1-^{13}C]lactate group ($p<0.05$, Student's t test).

Abbreviations: ALA, alanine; ASP, aspartate; CIT, citrate; GLN, glutamine; GLU, glutamate; MAL, malate; PYR, pyruvate; M+1, parent ion with one ^{13}C atom; M+2, parent ion with two ^{13}C atoms; M+3, parent ion with three ^{13}C atoms; M+4, parent ion with four ^{13}C atoms. *The enrichment detected in alanine derives directly from ^{13}C-labelled pyruvate and not from the TCA cycle when [1,6-^{13}C]glucose is the precursor. When [1,2-^{13}C]glucose is used, M+2 is not derived from the TCA cycle but M+1 alanine is. When [1,2-^{13}C]acetate is in the medium, both alanine isotopologues are derived from the TCA cycle

Figure 4 - [1-^{13}C]lactate metabolism and evidence for pyruvate carboxylation in oligodendrocytes. (A) Labelling patterns resulting from the metabolism of [1-^{13}C]lactate (^{13}C atoms are identified in red): [1-^{13}C]lactate (LAC) is converted into [1-^{13}C]pyruvate, which can be converted into acetyl-CoA via pyruvate dehydrogenase (PDH) or into [1-^{13}C]oxaloacetate (OAA) via pyruvate carboxylase (PC). The first carbon of pyruvate is lost in its conversion to acetyl-CoA via PDH. Therefore, the ^{13}C label can only be observed downstream of pyruvate if PC is active. [1-^{13}C]oxaloacetate can condense with acetyl-CoA to form [6-^{13}C]citrate which also leads subsequently to the formation of unlabelled α-ketoglutarate by loss of carbon 6. (B) The % enrichment of ^{13}C in citrate indicates the contribution of pyruvate carboxylation to citrate formation from [1-^{13}C]lactate. The % of M+1 citrate was assessed using GC-MS in samples of cell extracts and culture medium from differentiated oligodendrocytes and also in cultures of cortical astrocytes after 24h of incubation with [1-^{13}C]lactate (oligodendrocytes - mean ± s.e.m., n=9; and astrocytes - mean ± s.e.m., n=6). (C) Contribution of pyruvate carboxylation to glutamate synthesis from [1,2-^{13}C]glucose. Oligodendrocytes were incubated in medium containing [1,2-^{13}C]glucose for 24h, extracted, and analysed using ^{13}C-magnetic resonance spectroscopy for the presence of isotopologues of glutamate formed via pyruvate carboxylation. The C-2 region of glutamate (GLU) at 55.5 ppm is shown. The doublet representing [2,3-^{13}C]glutamate is formed via pyruvate carboxylation and the doublet representing [1,2-^{13}C]glutamate is formed via pyruvate dehydrogenation. Abbreviations: ASP, aspartate; GLN, glutamine; GLU, glutamate; MAL, malate; OAA, oxaloacetate; PC, pyruvate carboxylase; PDH, pyruvate dehydrogenase; PYR, pyruvate.

Figure 5 – Integration of metabolic pathways operating in oligodendrocytes in the context of metabolic interactions with astrocytes and neurons/axons. The pathways investigated in the present study are highlighted in red in the oligodendrocyte: glucose is taken up and subsequently metabolized either via glycolysis only (1) or also via the pentose phosphate pathway (2); the resulting pyruvate (PYR) produced can be reduced to lactate (LAC) (3) which can be released and taken up by cells with lower lactate concentration. Moreover, pyruvate can be carboxylated via pyruvate carboxylase (PC) or malic enzyme (ME) into oxaloacetate (OAA) or malate (MAL) or enter the TCA cycle after being converted to acetyl CoA (Ac-CoA) via pyruvate dehydrogenase (PDH) (4). The TCA cycle intermediate α-ketoglutarate (α-KG) gives rise to glutamate (GLU) and, subsequently, glutamine (GLN), but none of these aminoacids appear to be significantly released. Pyruvate can be further completely oxidized if it is decarboxylated via ME, a pathway called pyruvate recycling (5), which also seems to be present in this cell type. Oligodendrocytes can also metabolise acetate into acetyl CoA (6) that can be then incorporated into lipids or oxidized in the TCA cycle.

Supplementary Figure 1 – Time courses of [1,6-^{13}C]glucose-derived percent enrichment of ^{13}C in intracellular alanine, citrate, malate, aspartate, glutamate and glutamine after 0, 4, 8 and 24h of incubation (n=12). M+1, parent ion with one ^{13}C atom; M+2, parent ion with two ^{13}C atoms; M+3, parent ion with three ^{13}C atoms. For labelling patterns see Figure 3A.